

# Secret Interactions of Sterile Neutrinos and MeV-scale gauge boson

Zahra Tabrizi<sup>1,2,\*</sup> and O. L. G. Peres<sup>2,3,1,†</sup>

<sup>1</sup>*School of Particles and Accelerators, Institute for Research in Fundamental Sciences (IPM), P.O.Box 19395-1795, Tehran, Iran*

<sup>2</sup>*Instituto de Física Gleb Wataghin - UNICAMP, 13083-859, Campinas, SP, Brazil*

<sup>3</sup>*Abdus Salam International Centre for Theoretical Physics, ICTP, I-34010, Trieste, Italy*

(Dated: July 10, 2022)

Recent results from neutrino experiments show evidence for light sterile neutrinos which do not have any Standard Model interactions. These light sterile states are disfavored by cosmology due to the constraints from the Big Bang Nucleosynthesis and Large Scale Structure Formation. This tension could be solved if the sterile neutrino states had Secret Interaction with a light gauge boson  $X$  with mass  $M_X$  and coupling  $g_X$ , and with a field strength at least  $10^3 - 10^4$  times larger than the Fermi constant. We show that such large interaction strength is ruled out due to the constraints from MINOS experiment. By performing an analysis on the Secret Interaction of the sterile neutrinos using the MINOS data and comparing with the results of cosmology, the CCFR experiment and the  $(g-2)_\mu$  data we have found a concordance region for  $g_X \sim (4-8) \times 10^{-4}$  and  $M_X \sim (10-24)$  MeV.

PACS numbers: 14.60.Lm, 14.60.St, 14.60.Pq

## INTRODUCTION

Most of the data collected from the neutrino oscillation experiments are in agreement with the 3 neutrino hypothesis [1]. However, the observation of the reactor anomalies, which is a deficit of electron anti-neutrinos produced in the reactors [2, 3], together with the results of the MiniBooNE experiment [4] which shows evidence for  $\nu_\mu \rightarrow \nu_e$  conversion, cannot be explained by the usual 3 neutrino scenario [5]. The most popular way to clarify these anomalies is to assume there exists 1 (or more) neutrino state(s) which does not have any weak interaction (therefore is sterile), but can mix with the active neutrinos in the Standard Model (SM) and change their oscillation behavior pattern. In the minimal "3+1" model [6] the flavor and mass eigenstates of neutrinos are related through the unitary  $(3+1) \times (3+1)$  PMNS matrix  $U$ :  $\nu_\alpha = \sum_{i=1}^{3+1} U_{\alpha i}^* \nu_i$ . The oscillation probability of neutrinos is described using the active-active and active-sterile mixing angles, as well as the mass squared differences  $\Delta m_{21}^2$ ,  $\Delta m_{31}^2$  and  $\Delta m_{41}^2$ , where  $\Delta m_{ij}^2 \equiv m_i^2 - m_j^2$ .

Although most of the anomalies seen in the neutrino sector are in favor of the sterile models with the mass squared difference  $\Delta m_{41}^2 \sim 1 \text{ eV}^2$ , there are conflicts between the sterile hypothesis and cosmology. Such light additional sterile states thermalize in the early universe through their mixing with the active neutrinos; therefore, we effectively have additional relativistic number of neutrinos which can be parametrized by  $\Delta N_{\text{eff}}$ . In the standard model of cosmology we have  $\Delta N_{\text{eff}} = 0$ . Massive sterile neutrinos with mass  $\sim 1 \text{ eV}$  and large enough mixing angles to solve the reactor anomalies imply full thermalization at the early universe. This means that for any additional species of sterile neutrinos, we should have  $\Delta N_{\text{eff}} = 1$ . However, this is not consistent with the Big Bang Nucleosynthesis and the Planck results, which state  $\Delta N_{\text{eff}} < 0.7$  with 90% C.L. [7]. It was recently

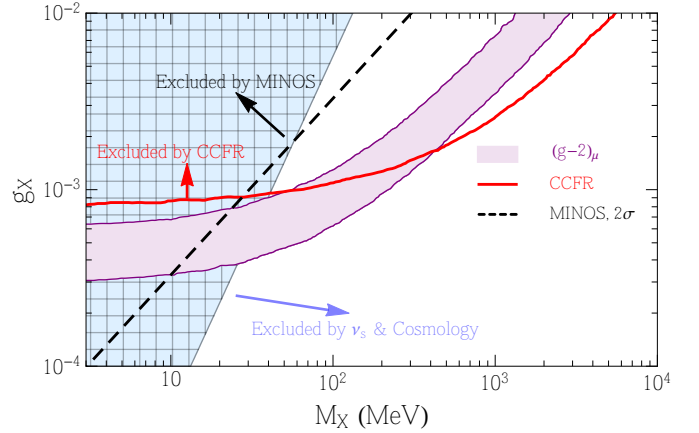


FIG. 1. We have shown the region of interest for the  $\nu_s$ SI model with a light gauge boson with coupling  $g_X$  and mass  $M_X$ . The result of the analysis of the  $\nu_s$ SI model with the MINOS data is shown by the black dashed curve with  $2\sigma$  C.L.. The red curve is the constraint from Ref. [10], using the data of the CCFR experiment [11], while the purple shaded region is the constraint from  $(g-2)_\mu$  [10]. The blue shaded region is where the tension between the sterile neutrino and cosmology is relieved due to the presence of the  $\nu_s$ SI model [8, 9].

proposed in [8, 9] that this problem could be solved if the sterile neutrino state interacts with a new gauge boson  $X$  with mass  $\sim$  a few MeV. This can easily produce a large field strength for the sterile neutrinos. In this way the sterile state experiences a large thermal potential which suppresses the mixing between the active and sterile states in the early universe. Therefore, the abundance of the sterile neutrinos remains small, and its impact on the Big Bang nucleosynthesis (BBN), Cosmic Microwave Background (CMB) and the Large Scale Structure Formation would be negligible, hence the sterile state can be consistent with the cosmological model.

In this work we investigate the possibility of the sterile

neutrino states interacting with a new gauge boson  $X$ , with mass  $\sim \text{MeV}$ , which has coupling with the sterile neutrinos and the charged leptons in the SM. This new interaction of the sterile neutrinos was first mentioned in [12]. The " $\nu_s$  *Secret Interaction*" ( $\nu_s$ SI) model produces a neutral current (NC) matter potential for the sterile states proportional to  $G_X$ , where  $G_X$  is the field strength of the new interaction. The NC matter potential in the  $\nu_s$ SI model changes the oscillation probability of neutrinos and anti-neutrinos drastically. Therefore, using the data of a neutrino oscillation experiment such as the MINOS experiment [13], we can test the  $\nu_s$ SI model. On the other hand, we can also use the data of the MINOS experiment to constrain the mass of the light gauge boson in the  $\nu_s$ SI model.

We summarize all results in Fig. (1). In this figure we have shown the region of interest for the  $\nu_s$ SI model with coupling  $g_X$  and mass  $M_X$ . The analysis of the MINOS data on the  $\nu_s$ SI model is shown by the black dashed curve, which disallows the values of  $G_X/G_F > 92.4$  at  $2\sigma$  C.L., where  $G_F$  is the Fermi constant. The red solid curve shows the constraint from the CCFR experiment [11]. The purple shaded region is the  $(M_X - g_X)$  region allowed from the  $(g-2)_\mu$  data [10]. The blue shaded region shows the condition that prevents the thermalization of the sterile neutrinos in the early universe.

## THE FORMALISM

We enlarge the SM with one extra species of the sterile neutrinos which do not couple with the SM gauge bosons, but have interactions with a new  $U_X(1)$  gauge symmetry (the  $\nu_s$ SI model). The sterile neutrinos couple with the  $X$  boson with the coupling constant  $g_X$ . The strength of this new interaction is given by

$$G_X = \frac{g_X^2}{M_X^2}, \quad (1)$$

where  $M_X$  is the mass of the new gauge boson. The active neutrinos of the SM have charged and neutral current interactions with the  $W^\pm$  and  $Z$  bosons. Their matter potential is therefore given by  $V_\alpha(r) = \delta_{\alpha e} V_{CC}(r) + V_{NC}(r) = \sqrt{2}G_F N_e(r)(\delta_{\alpha e} - 1/2)$ , where  $\alpha = e, \mu, \tau$  and  $V_{CC(NC)}$  is the charged (neutral) current potential of the active neutrinos. The factor  $G_F$  is the Fermi constant, while  $N_e(r)$  is electron number density of the earth given by the PREM model [14]. We have assumed that the electron and neutron number densities are equal for our practical purposes.

The sterile neutrinos which couple to the  $X$  boson will also have neutral current matter potential which is proportional to the strength field of the new interaction:

$$V_s(r) = -\frac{\sqrt{2}}{2}G_X N_e(r) \equiv \alpha V_{NC}(r), \quad (2)$$

where the dimensionless parameter  $\alpha$  is defined as

$$\alpha = \frac{G_X}{G_F}. \quad (3)$$

For  $\alpha \rightarrow 0$  we recover the minimal  $3 + 1$  sterile neutrino model.

The evolution of neutrinos in the  $\nu_s$ SI model can be found by solving the following Schrödinger-like equation

$$i \frac{d}{dr} \begin{pmatrix} \nu_e \\ \nu_\mu \\ \nu_\tau \\ \nu_s \end{pmatrix} = \left[ \frac{1}{2E_\nu} U M^2 U^\dagger + V^{\nu_s \text{SI}}(r) \right] \begin{pmatrix} \nu_e \\ \nu_\mu \\ \nu_\tau \\ \nu_s \end{pmatrix}, \quad (4)$$

where  $U$  is the  $4 \times 4$  PMNS matrix [5], which is parametrized by the active-active mixing angles  $(\theta_{12}, \theta_{13}, \theta_{23})$  as well as 3 active-sterile mixing angles  $(\theta_{14}, \theta_{24}, \theta_{34})$ . The matrix

$$M^2 = \text{diag}\left(0, \Delta m_{21}^2, \Delta m_{31}^2, \Delta m_{41}^2\right)$$

is the matrix of the mass squared differences. Using Eq. (2), the matter potential matrix in the  $\nu_s$ SI model will be (after subtracting the constant  $V_{NC}(r) \times \mathbb{I}$ )

$$V^{\nu_s \text{SI}}(r) = \text{diag}\left(V_{CC}(r), 0, 0, V_s(r) - V_{NC}(r)\right) \\ = \sqrt{2}G_F N_e(r) \text{diag}\left(1, 0, 0, \frac{(1-\alpha)}{2}\right). \quad (5)$$

The same evolution equation applies to anti-neutrinos with the replacement  $V^{\nu_s \text{SI}}(r) \rightarrow -V^{\nu_s \text{SI}}(r)$ . We consider the  $\nu_s$ SI model with  $\alpha > 0$ . The so called MSW resonance condition [15] happens when

$$\frac{1}{2E_\nu} U M^2 U^\dagger = V^{\nu_s \text{SI}}(r). \quad (6)$$

Hence, for positive values of  $\Delta m_{ij}^2$ , the condition happens for neutrinos, not for anti-neutrinos.

One interesting place to test the  $\nu_s$ SI model is the MINOS long-baseline neutrino experiment [13]. The MINOS experiment which has a baseline of 735 km detects both muon and anti-muon neutrinos, and it is one of few experiments that is both sensitive to neutrino and anti-neutrino oscillation probabilities. For the baseline and energy range of the MINOS experiment, the oscillation probabilities of the neutrinos and anti-neutrinos are very similar in the usual 3 neutrino scenario. However, this does not hold in the  $\nu_s$ SI model anymore.

To see how the  $\nu_s$ SI model affects the oscillation probability of neutrinos, we compute the full numerical survival probabilities for muon (anti-)neutrino in the case of the standard 3 neutrino scenario and in the  $3 + 1$  and  $\nu_s$ SI models. We show in Fig. (2) the survival probability of  $\nu_\mu$  (top) and  $\bar{\nu}_\mu$  (bottom) for the standard 3 neutrino case (black dashed curve), the  $3 + 1$  model with  $\alpha = 0$  (red solid curve) and the  $\nu_s$ SI model with  $\alpha = 150$  (the

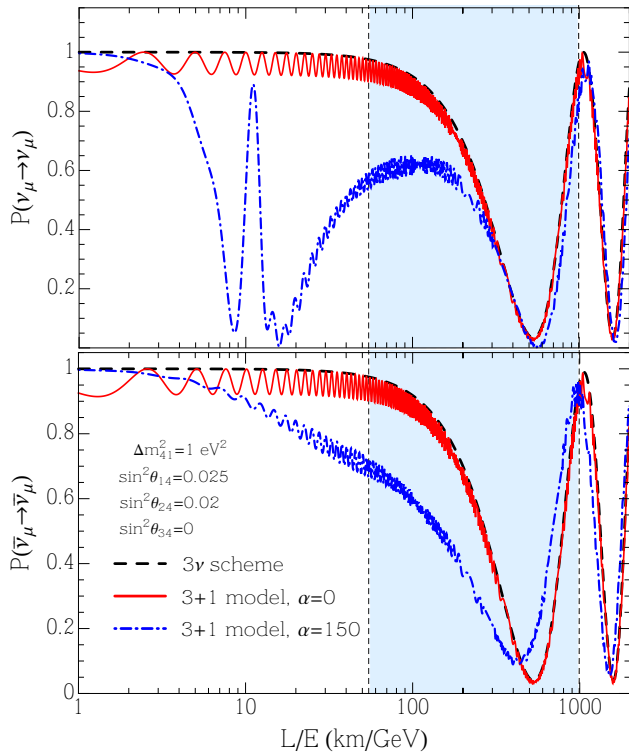


FIG. 2. The muon neutrino and anti-neutrino survival probabilities as a function of distance over neutrino energy are shown in the top and bottom, respectively. The black-dashed and the red-solid curves correspond to the 3 and 3+1 neutrino models, respectively. The blue dot-dashed curves represent the probabilities calculated in the  $\nu_s$ SI model for  $\alpha = 150$ . The standard 3 neutrino parameters are fixed by the NUFIT best fit values [16] and the active-sterile mixing parameters are shown in the plot. The blue shaded area is the range of  $L/E$  for the MINOS experiment [13].

blue dot-dashed curve). To calculate the probabilities, we have fixed the 3 neutrino oscillation parameters by the best fit values of NUFIT [16]:  $\Delta m_{21}^2 = 7.5 \times 10^{-5} \text{ eV}^2$ ,  $\Delta m_{31}^2 = 2.4 \times 10^{-3} \text{ eV}^2$ ,  $\sin^2 \theta_{12} = 0.3$ ,  $\sin^2 \theta_{23} = 0.6$  and  $\sin^2 \theta_{13} = 0.023$ . The values of the active-sterile mixing parameters in the 3+1 and  $\nu_s$ SI models are listed in Figure (2) [5]. Comparing the 3 neutrino case (the black dashed curve) with the 3+1 model (the red solid curve), we see that the effect of the sterile neutrino with mass squared difference  $\Delta m_{41}^2 = 1 \text{ eV}^2$  is marginal adding only a very fast oscillation on the top of the oscillation induced by the atmospheric mass squared difference  $\Delta m_{31}^2$ . In the  $\nu_s$ SI model we have dramatic effects both for neutrino and anti-neutrino survival probabilities. When the resonance condition applies (Eq. (6)), we expect stronger changes for the  $\nu_\mu$  survival probability, while for anti-neutrinos the changes are milder. This can be seen in the blue dot-dashed curve at the top and bottom of Fig. (2).

## THE ANALYSIS

We analyze the collected  $\nu_\mu$  and  $\bar{\nu}_\mu$  beam data in the MINOS experiment to constrain the  $\alpha$  parameter in the  $\nu_s$ SI model. We calculate the expected number of events in each bin of energy by

$$N_i^{\text{osc}}(s_{23}^2, s_{24}^2, \Delta m_{31}^2, \Delta m_{41}^2; \alpha) = N_i^{\text{no-osc}} \times \langle P_{\text{sur}}(s_{23}^2, s_{24}^2, \Delta m_{31}^2, \Delta m_{41}^2; \alpha) \rangle_i, \quad (7)$$

where  $s_{ij}^2 \equiv \sin^2 \theta_{ij}$  and  $N_i^{\text{no-osc}}$  is the expected number of events for no-oscillation case in the  $i$ th bin of energy after subtracting background [13]; while  $\langle P_{\text{sur}}(s_{23}^2, s_{24}^2, \Delta m_{31}^2, \Delta m_{41}^2; \alpha) \rangle_i$  is the averaged  $\nu_\mu \rightarrow \nu_\mu$  ( $\bar{\nu}_\mu \rightarrow \bar{\nu}_\mu$ ) survival probability in the  $i$ th energy bin, calculated using Eq. (4) for the fixed values  $\sin^2 \theta_{14} = 0.025$  and  $\sin^2 \theta_{34} = 0$  and letting the other parameters to vary.

To analyze the full MINOS data we define the following  $\chi^2$  function

$$\chi^2(a, b, s_{23}^2, s_{24}^2, \Delta m_{31}^2, \Delta m_{41}^2; \alpha) = \sum_i \frac{[(1+a)N_i^{\text{osc}} + (1+b)N_i^b - N_i^{\text{obs}}]^2}{(\sigma_i^{\text{obs}})^2} + \frac{a^2}{\sigma_a^2} + \frac{b^2}{\sigma_b^2}, \quad (8)$$

where  $i$  runs over the bins of energy (23 for  $\nu_\mu$  events and 12 for  $\bar{\nu}_\mu$  events),  $N_i^{\text{osc}}$  is the expected number of events defined in Eq. (7),  $N_i^b$  and  $N_i^{\text{obs}}$  are the background and observed events, respectively. The  $\sigma_i^{\text{obs}} = \sqrt{N_i^{\text{obs}}}$  represents the statistical error of the observed events. The parameters  $a$  and  $b$  take into account the systematic uncertainties of the normalization of the neutrino flux and the background events respectively, with  $\sigma_a = 0.016$  and  $\sigma_b = 0.2$ .

After combining the  $\chi^2$  function for the  $\nu_\mu$  and  $\bar{\nu}_\mu$  events and marginalizing over all parameters, we find the following best fit values:  $\Delta m_{31}^2 = 2.43 \times 10^{-3} \text{ eV}^2$ ,  $\Delta m_{41}^2 = 4.35 \text{ eV}^2$ ,  $s_{23}^2 = 0.67$ ,  $s_{24}^2 = 0.03$ , and  $\alpha = 19.95$ , while the ratio of the  $\chi^2$  value over the number of degrees of freedom is  $\chi^2/\text{d.o.f} = 39.7/30$ . When we increase  $\alpha$  from its best fit value we have disagreement between the  $\nu_s$ SI model and the MINOS data. From this we can find an upper bound for  $\alpha$  at  $2\sigma$  C.L.:

$$\alpha < 92.4. \quad (9)$$

Using Eq. (1) and Eq. (3) we can write down the coupling  $g_X$  as a function of the gauge boson mass  $M_X$  and for the fixed value of  $\alpha$  by the following relation :

$$g_X = \sqrt{\alpha G_F} M_X = 3 \times 10^{-5} \sqrt{\frac{\alpha}{92.4}} \left( \frac{M_X}{\text{MeV}} \right). \quad (10)$$

Therefore, we can use the expression above to find an exclusion region in the  $(M_X - g_X)$  plane. The black

dashed curve in Fig. (1) shows the allowed region in the  $\nu_s$ SI model using the data of the MINOS experiment.

To compare the results of this analysis with other constraints, we show in Fig. (1) the negative impact of the presence of light gauge boson [10] with the red solid curve, using the data of the CCFR experiment [11]. The experimental result of the  $(g-2)_\mu$  value is more than  $3\sigma$  far from the SM prediction [17]. One of the possible explanations is the presence of an "MeV-scale" gauge boson. The purple shaded region in Fig. (1) shows the constraint from  $(g-2)_\mu$  [10].

The sterile neutrino states with 1 eV mass have dramatic effects in cosmology due to their thermalization in the early universe, and they are disfavored by the Planck data. This tension could be removed if  $V_{\text{eff}} \gg \frac{\Delta m_{41}^2}{2E}$  [9, 18, 19], where  $V_{\text{eff}}$  is the effective temperature dependent potential of the sterile neutrinos in the early universe. The blue shaded region in Fig. (1) shows this condition at the time of BBN ( $E \simeq T_s \simeq 1$  MeV). To translate this condition in the context of the  $\nu_s$ SI model, the  $\alpha$  parameter should be at least as large as  $10^3-10^4$  [8].

When we compare the result of our analysis on the  $\nu_s$ SI model with the  $(g-2)_\mu$  constraint, we find that values of  $M_X < 10$  MeV are excluded with  $2\sigma$  C.L.. On the other hand, combining our result with the CCFR experiment we find that  $g_X < 9 \times 10^{-4}$  with  $2\sigma$  C.L..

Finally, as can be seen from Fig. (1), after we combine the result of this work with the constraints found from the CCFR experiment,  $(g-2)_\mu$  and cosmology, there is only a very tiny region in the  $(M_X - g_X)$  plane which is allowed by all experimental bounds for  $g_X \sim (4-8) \times 10^{-4}$  and  $M_X \sim (10-24)$  MeV.

The "MeV scale" gauge bosons have been studied widely in the literature, for example, the  $L_\mu - L_\tau$  symmetry [10] and the  $B - L$  inspired model [20]. Studying the phenomenological details of these models is beyond the scope of this work and is left for a future analysis.

## CONCLUSIONS

An interesting interplay between the information from cosmology and from neutrino oscillation experiments allows us to test the presence of new interaction of an "MeV scale" gauge boson with the sterile neutrinos. We called this model the Secret Interaction of sterile neutrinos ( $\nu_s$ SI) model, where the coupling constant of this model is  $g_X$  and the mass of the light gauge boson is  $M_X$ . The conflict between the thermalization of the sterile neutrinos in the early universe and cosmology can be solved if the sterile states interact with this light gauge boson  $X$ . In this paper we studied the  $\nu_s$ SI model using the data of the MINOS neutrino experiment and showed that the values above  $\alpha = G_X/G_F = 92.4$  are excluded.

We combined the result of this paper on the  $\nu_s$ SI model

using the MINOS data with the information from the CCFR experiment, the  $(g-2)_\mu$  data and the constraint from cosmology and found that there is only a tiny allowed region in the  $(M_X - g_X)$  plane which agrees with all constraints. For this region we found  $g_X \sim (4-8) \times 10^{-4}$  and  $M_X \sim (10-24)$  MeV which correspond to a field strength of  $G_X \sim (70-90)G_F$ . We can use the data of the future neutrino oscillation experiments such as the DUNE experiment [21, 22] to test such strong field strength and get a definite answer on the presence of the light gauge boson.

## ACKNOWLEDGMENTS

Z. T. thanks the hospitality of UNICAMP and O. L. G. P thanks the hospitality of IPM. O. L. G. P. thanks the support of FAPESP funding grant 2012/16389-1.

---

\* tabrizi.physics@ipm.ir

† orlando@ifi.unicamp.br

- [1] M. C. Gonzalez-Garcia and Y. Nir, Rev.Mod.Phys. **75**, 345 (2003).
- [2] G. Mention *et al.*, Phys. Rev. D **83**, 073006 (2011).
- [3] P. Huber, Phys. Rev. C **84**, 024617 (2011).
- [4] A. A. Aguilar-Arevalo *et al.* (MiniBooNE Collaboration), Phys. Rev. Lett. **105**, 181801 (2010).
- [5] K. N. Abazajian *et al.*, (2012), arXiv:1204.5379.
- [6] O. L. G. Peres and A. Y. Smirnov, Nucl.Phys. **B599**, 3 (2001).
- [7] P. A. R. Ade *et al.* (Planck), (2015), arXiv:1502.01589.
- [8] S. Hannestad, R. S. Hansen, and T. Tram, Phys.Rev.Lett. **112**, 031802 (2014).
- [9] B. Dasgupta and J. Kopp, Phys.Rev.Lett. **112**, 031803 (2014).
- [10] W. Altmannshofer, S. Gori, M. Pospelov, and I. Yavin, Phys.Rev.Lett. **113**, 091801 (2014).
- [11] S. R. Mishra *et al.* (CCFR), Phys.Rev.Lett. **66**, 3117 (1991).
- [12] M. Pospelov, Phys.Rev. **D84**, 085008 (2011).
- [13] P. Adamson *et al.* (MINOS Collaboration), Phys. Rev. Lett. **110**, **251801** (2013).
- [14] A. M. Dziewonski and D. L. Anderson, Physics of the Earth and Planetary Interiors **25**, 297 (1981).
- [15] S. P. Mikheyev and A. Y. Smirnov, Sov. Jour. Nucl. Phys. **42**, 913 (1985).
- [16] M. C. Gonzalez-Garcia, M. Maltoni, J. Salvado, and T. Schwetz, JHEP **12**, 123 (2012).
- [17] T. P. Gorringer and D. W. Hertzog, (2015), arXiv:1506.01465.
- [18] J. Kopp and J. Welter, JHEP **1412**, 104 (2014).
- [19] X. Chu, B. Dasgupta, and J. Kopp, (2015), arXiv:1505.02795 [hep-ph].
- [20] N. Engelhardt, A. E. Nelson, and J. R. Walsh, Phys. Rev. **D81**, 113001 (2010).
- [21] J. M. Berryman, A. de Gouvea, K. J. Kelly, and A. Kobach, (2015), arXiv:1507.03986 [hep-ph].
- [22] C. Adams *et al.* (LBNE), (2013), arXiv:1307.7335 [hep-ex].